Supplementary information

Effects of Bromine-Containing Counterion Salts in Directing the Structures of Medium-Sized Silver Nanoclusters†

Haoqi Li, Xiao Wei, Xi Kang,* Manzhou Zhu

Department of Chemistry and Centre for Atomic Engineering of Advanced Materials, Key Laboratory of Structure and Functional Regulation of Hybrid Materials of Ministry of Education, Institutes of Physical Science and Information Technology and Anhui Province Key Laboratory of Chemistry for Inorganic/Organic Hybrid Functionalized Materials, Anhui University, Hefei, Anhui 230601, China.

*E-mails of corresponding authors: kangxi_chem@ahu.edu.cn (X.K.)

This PDF file includes:

Experimental Methods

Materials

All reagents were purchased from Sigma-Aldrich and used without further purification, including silver nitrate ($AgNO_3$, 99.9%, metal basis), 1-adamantane thiol ($C_{10}H_{15}SH$, HS-Adm, 95%), diphenyl-2-pyridylphosphine ($C_{17}H_{14}NP$, 98%), borane-tert-butylamine complex ($C_4H_{14}BN$, 97%), tetraphenylphosphonium bromide (PPh_4Br, 99%), tetraoctylammonium bromide ($C_{32}H_{68}BrN$, TOABr, 98%)，methylene chloride (CH_2Cl_2, HPLC grade), methanol (CH_3OH, HPLC grade), and n-hexane (Hex, HPLC grade).

Synthesis of $[Ag_{52}(SR)_{30}Br_4H_{20}]^{2-}$ (Ag_{52}) and $[Ag_{54}(SR)_{30}Br_4H_{22}]^{2-}$ (Ag_{54})

94mg of $AgNO_3$ was dissolved in 5ml methanol, followed by the addition of a mixture consisting of 5ml methanol and 10ml ethanol. Stir the solution for 10 minutes, add 50mg of HS-Adm to achieve a green transparent solution. After an additional 10 minutes, upon adding 100mg diphenyl-2-pyridylphosphine, the solution starts to exhibit turbidity. Maintain stirring for another duration of ten minutes before sequentially introducing both the borane-tert-butylamine complex (100mg) and tetraphenylphosphonium bromide (50mg). Following a reaction time span of twelve hours, perform spin-evaporation under vacuum conditions and conduct two washes with methanol and *n*-hexane respectively to obtain Ag_{52} and Ag_{54} clusters. The yield is 45% based on the Ag element (calculated from the $AgNO_3$).

Synthesis of $[Ag_{58}(SR)_{30}Br_4 (NO_3)_2H_{22}]^{2+}$ (Ag_{58})

The synthesis of $[Ag_{58}(SR)_{30}Br_4 (NO_3)_2H_{22}]^{2+}$ was the same as that of $[Ag_{52}(SR)_{30}Br_4H_{20}]^{2-}$, except that PPh_4Br was replaced by TOABr. The yield is 20% based on the Ag element (calculated from the $AgNO_3$).

Crystallization of Ag_{52} and Ag_{54} nanoclusters

After 12 h of reaction, the mixture was rotationally evaporated under vacuum. They were washed twice each with methanol and hexane. Single crystals of these nanoclusters were cultivated at room temperature by liquid diffusion of *n*-hexane into a CH_2Cl_2 solution containing each nanocluster. After 14 days, yellow crystals were collected, and the structures of these nanoclusters were determined.

Crystallization of the Ag_{58} nanocluster

After 12 h of reaction, the mixture was rotationally evaporated under vacuum. They were washed twice each with methanol and hexane. Single crystals of the Ag_{58} nanocluster was cultivated at room temperature by liquid diffusion of *n*-hexane into a CH_2Cl_2 solution containing each nanocluster. After 14 days, brown crystals were collected.

X-ray crystallography

The data collection for single-crystal X-ray diffraction (SC-XRD) of all nanocluster crystal samples was carried out on Stoe Stadivari diffractometer under nitrogen flow, using graphite-monochromatized Cu Kα radiation (λ = 1.54186 Å). Data reductions and absorption corrections were performed using the SAINT and SADABS programs, respectively. The structure was solved by direct methods and refined with full-matrix least squares on F^2 using the SHELXTL software package. All non-hydrogen atoms were refined anisotropically, and all the hydrogen atoms were set in geometrically calculated positions and refined isotropically using a riding model. All crystal structures were treated with PLATON SQUEEZE, and the diffuse electron densities from these residual solvent molecules were removed. The CCDC number of the

$Ag_{52}(SR)_{30}Br_4$ nanocluster is 2301182. The CCDC number of $Ag_{54}(SR)_{30}Br_4$ is 2301180. The CCDC number of $Ag_{58}(SR)_{30}Br_4(NO_3)_2$ is 2301183.

Measurements

All UV-vis absorption spectra of the nanoclusters dissolved in CH_2Cl_2 were recorded using an Agilent 8453 diode array spectrometer.

Electrospray ionization mass spectrometry (ESI-MS) measurements were performed by Waters XEVO G2-XS QTof mass spectrometer. The sample was directly infused into the chamber at 5 µL/min. For preparing the ESI samples, nanoclusters were dissolved in CH_2Cl_2 (1 mg/mL) and diluted (*v*/*v* = 1:1) by CH_3OH.

Photoluminescence (PL) spectra were measured on an FL-4500 spectrofluorometer with the same optical density (OD) of ~0.1.

X-ray photoelectron spectroscopy (XPS) measurements were performed on a Thermo ESCALAB 250 configured with a monochromatized Al K*α* (1486.8 eV) 150 W X-ray source, a 0.5 mm circular spot size, a flood gun to counter charging effects, and an analysis chamber base pressure lower than 1×10^{-9} mbar.

Nuclear magnetic resonance (NMR) spectra are acquired using a Bruker 600 Avance III spectrometer equipped with a Bruker BBO multinuclear probe (BrukerBioSpin).

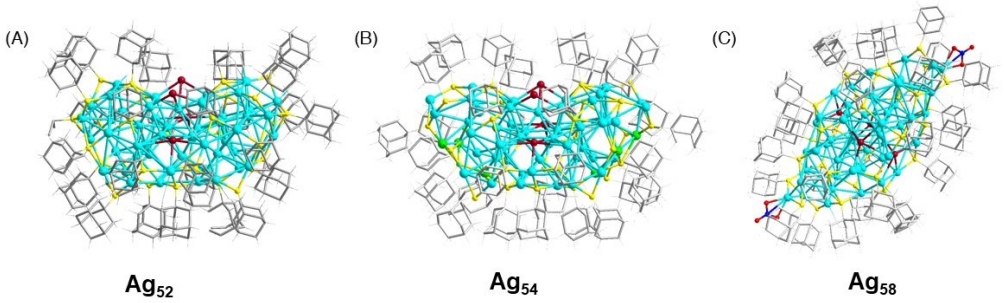

Figure S1. Crystal structures of nanoclusters in this work. (A) Crystal structure of the Ag_{52} nanocluster. (B) Crystal structure of the Ag_{54} nanocluster. (C) Crystal structure of the Ag_{58} nanocluster. Color labels: Light blue/green = Ag; yellow = S; brown = Br; blue= N; red = O; grey = C; white = H.

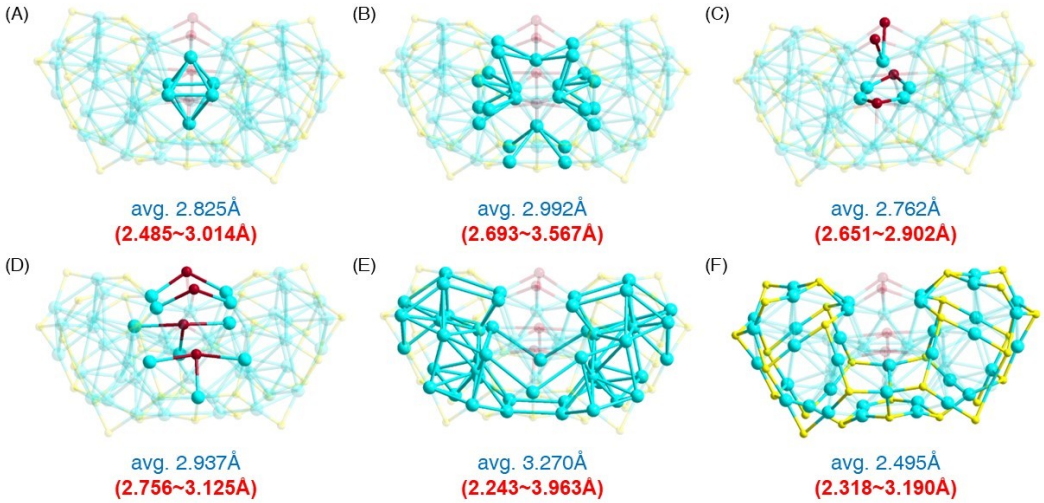

Figure S2. Comparison of the corresponding bond lengths in the Ag_{52} nanocluster. (A) Comparison of the length of Ag(octahedral surface)---Ag(octahedral surface) bonds. (B) Comparison of the length of Ag(octahedral surface)---Ag(motif) bonds. (C) Comparison of the length of Ag(octahedral surface)---Br bonds. (D) Comparison of the length of Br---Ag(motif) bonds. (E) Comparison of the length of Ag(motif)---Ag(motif) bonds. (F) Comparison of the length of Ag(motif)---S(motif) bonds. The compare bonds were highlighted for clarity.

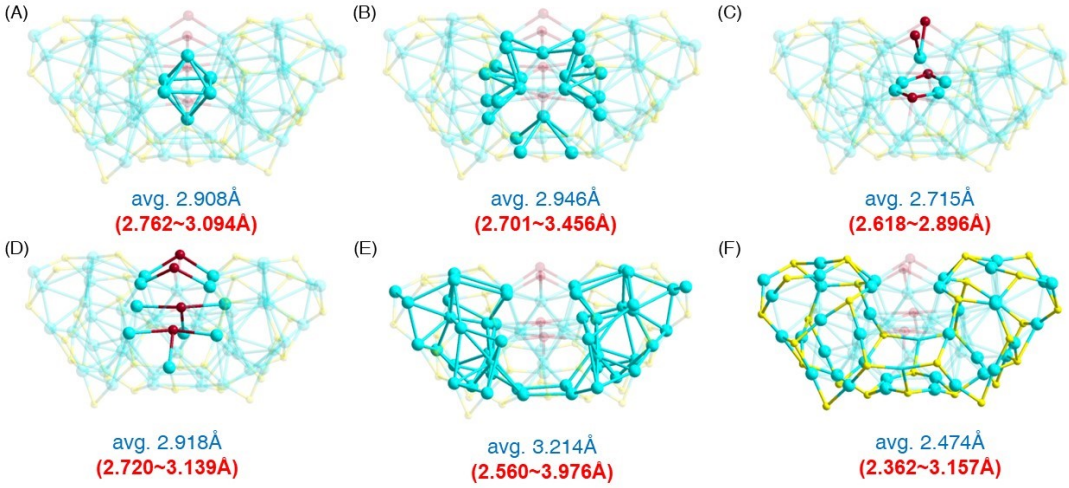

Figure S3. Comparison of the corresponding bond lengths in the Ag_{54} nanocluster. (A) Comparison of the length of Ag(octahedral surface)---Ag(octahedral surface) bonds. (B) Comparison of the length of Ag(octahedral surface)---Ag(motif) bonds. (C) Comparison of the length of Ag(octahedral surface)---Br bonds. (D) Comparison of the length of Br---Ag(motif) bonds. (E) Comparison of the length of Ag(motif)---Ag(motif) bonds. (F) Comparison of the length of Ag(motif)---S(motif) bonds. The compare bonds were highlighted for clarity.

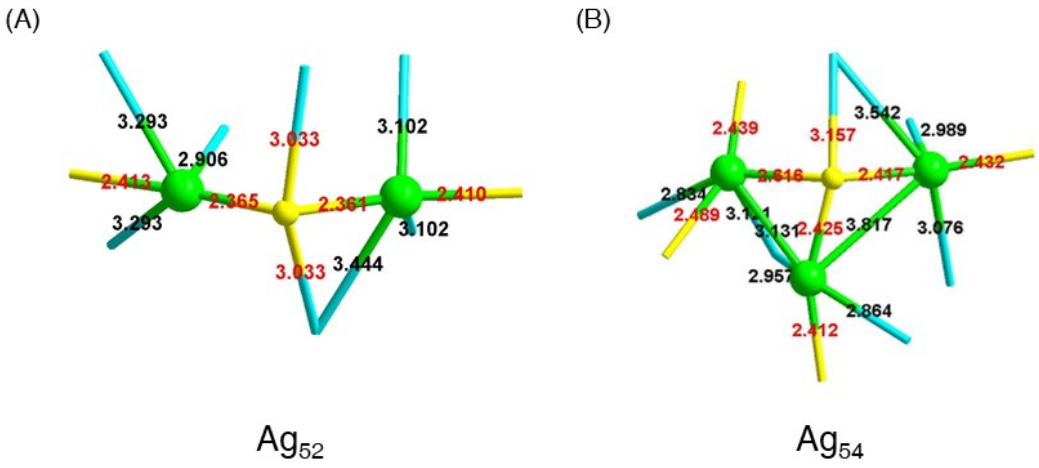

Figure S4. Comparison of bond lengths in $Ag_2(SR)_1$ motif in Ag_{52} clusters and $Ag_3(SR)_1$ motif in Ag_{54} clusters. Among them, the red font is the Ag-S bond length, and the black font is the Ag-Ag bond length. Color labels: green = Ag; yellow = S. All C and H atoms were omitted for clarity.

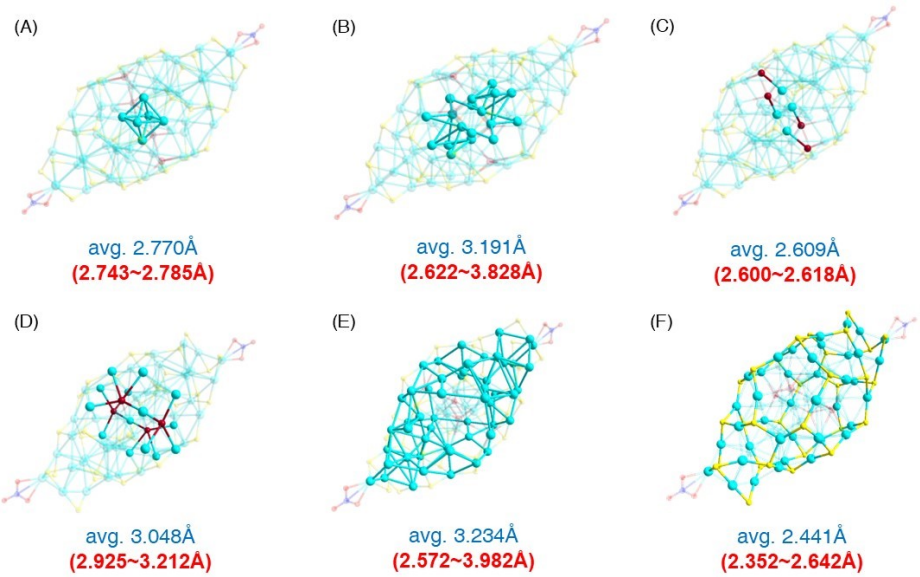

Figure S5. Comparison of the corresponding bond lengths in the Ag_{58} nanocluster. (A) Comparison of the length of Ag(octahedral surface)---Ag(octahedral surface) bonds. (B) Comparison of the length of Ag(octahedral surface)---Ag(motif) bonds. (C) Comparison of the length of Ag(octahedral surface)---Br bonds. (D) Comparison of the length of Br---Ag(motif) bonds. (E) Comparison of the length of Ag(motif)---Ag(motif) bonds. (F) Comparison of the length of Ag(motif)---S(motif) bonds. The compare bonds were highlighted for clarity.

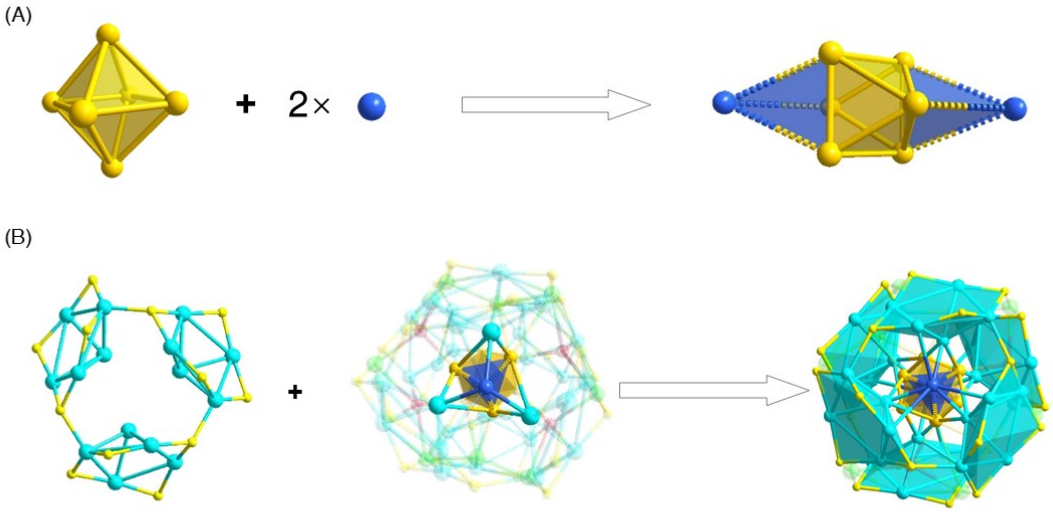

Figure S6. The structure of Ag_8 unit and Ag_{46} unit is formed. (A) At both ends of the Ag_6 core, two polar Ag atoms (marked in blue) were symmetrically connected to two Ag_3 surfaces in the Ag_6 octahedron, forming two Ag_4 tetrahedra and constituting the Ag_8 structure. (B) The three exposed Ag_3 surfaces (blue surfaces) of the two Ag_4 tetrahedra were connected to an $Ag_5(SR)_4$ motif, forming the $Ag_{46}(SR)_{24}Br_4$ unit. Color labels: gold/blue/light blue = Ag; yellow = S; brown = Br. All C and H atoms were omitted for clarity.

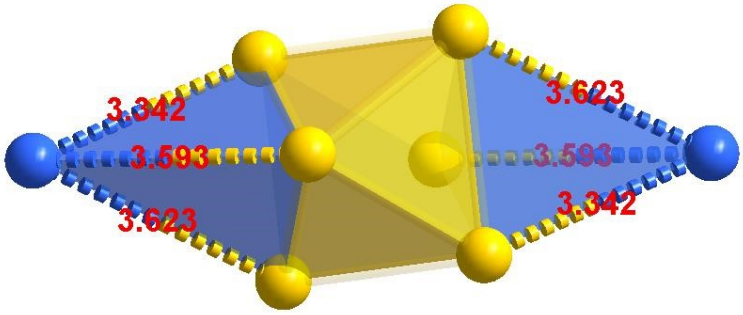

Figure S7. Bond length between polar Ag atom and Ag_6 core. Color labels: gold/ blue = Ag.

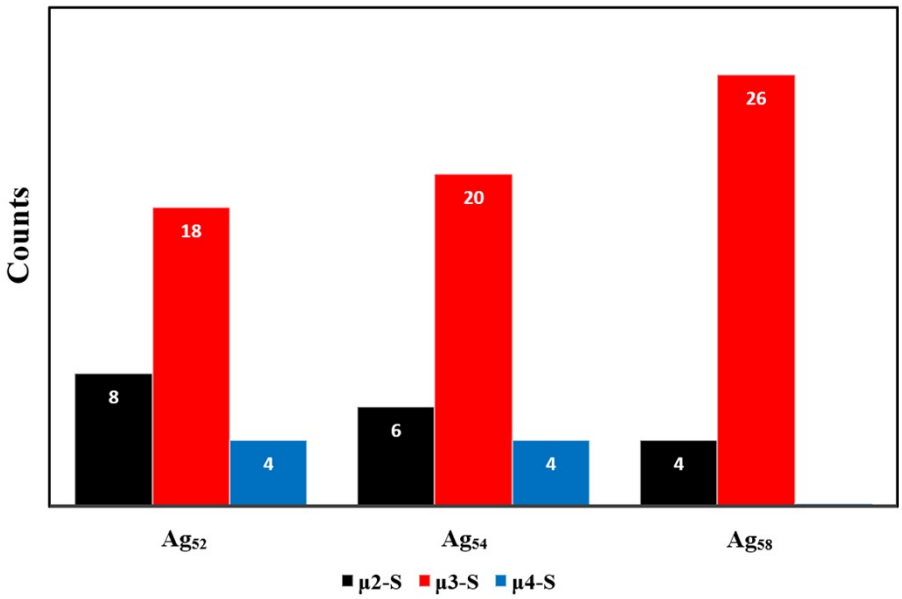

Figure S8. Comparison of the numbers of μ_2-S、μ_3-S and μ_4-S in Ag_{52}, Ag_{54}, and Ag_{58} nanoclusters. The number of μ_2-S was decreased from Ag_{52} to Ag_{54} and Ag_{58}. The number of μ_3-S was increased from Ag_{52} to Ag_{54} and Ag_{58}. It is worth noting that there are only μ_2-S and μ_3-S in Ag_{58}.

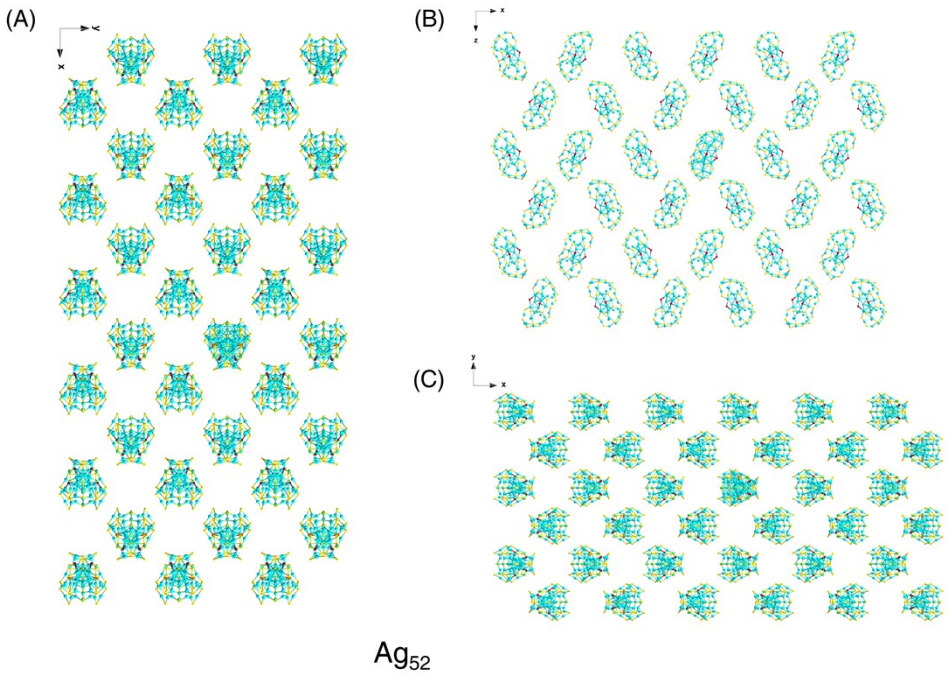

Figure S9. Packing of Ag_{52} nanoclusters in the crystal lattice: view from the *x* axis (A), *y* axis (B) and *z* axis (C). Color labels: Light blue/green = Ag; yellow = S; brown = Br. All C and H atoms were omitted for clarity.

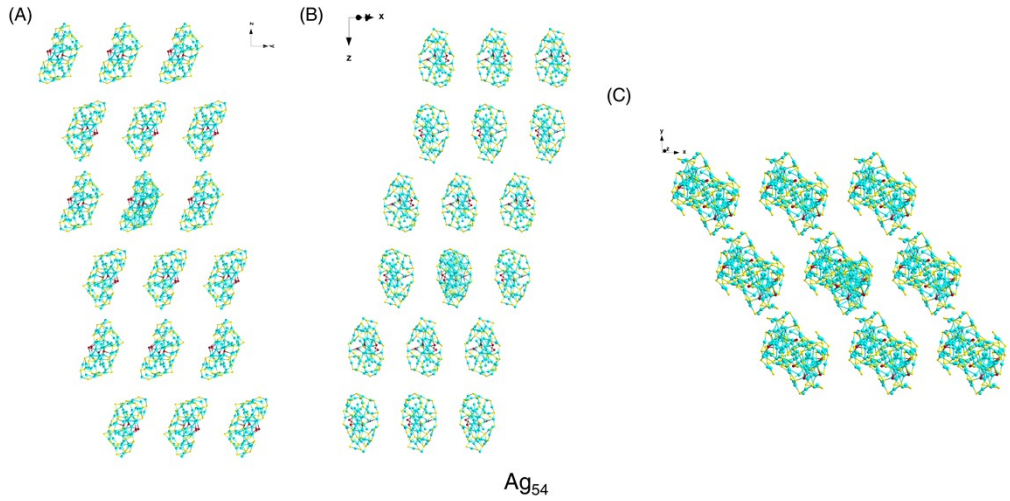

Figure S10. Packing of Ag_{54} nanoclusters in the crystal lattice: view from the *x* axis (A), *y* axis (B) and *z* axis (C). Color labels: Light blue/green = Ag; yellow = S; brown = Br. All C and H atoms were omitted for clarity.

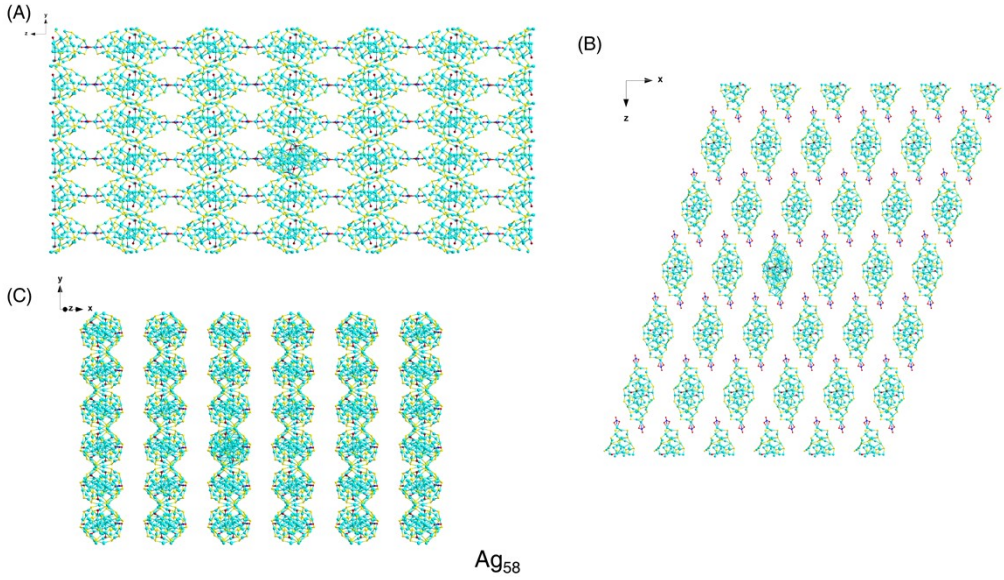

Figure S11. Packing of Ag_{58} nanoclusters in the crystal lattice: view from the *x* axis (A), *y* axis (B) and *z* axis (C). Color labels: Light blue/green = Ag; yellow = S; brown = Br; blue= N; red = O. All C and H atoms were omitted for clarity.

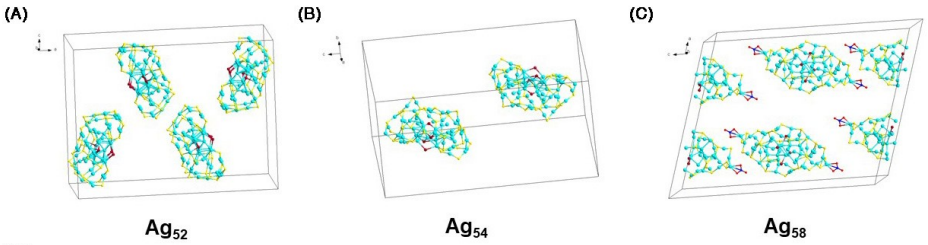

(D)

	Ag_{52}	Ag_{54}	Ag_{58}
Crystal System	orthorhombic	triclinic	monoclinic
Space Group	Pnma	*P -1*	*C 2/c*
a,b,c/Å	a=47.2631(8) b=24.0336(3) c=35.4451(4)	a=21.8845(2) b=22.1526(3) c=49.1884(4)	a=38.5120(6) b=21.9660(4) c=49.9423(9)
α,β,γ/°	α=90 β=90 γ=90	α=91.508(1) β=101.282(1) γ=118.372(1)	α=90 β=107.332(1) γ=90
Volume/Å^3	40262.17(96)	20379.04(44)	40330.59(123)
Density(gcm^{-1})	1.76438	1.81891	1.92984
z	4	2	4

Figure S12. Crystal lattices of (A) Ag_{52} (B) Ag_{54} and (C) Ag_{58} nanoclusters. (D) Comparison of the crystalline unit cell parameters of Ag_{52} Ag_{54} and Ag_{58} nanoclusters. Color labels: Light blue/green = Ag; yellow = S; brown = Br; blue= N; red = O. All C and H atoms were omitted for clarity.

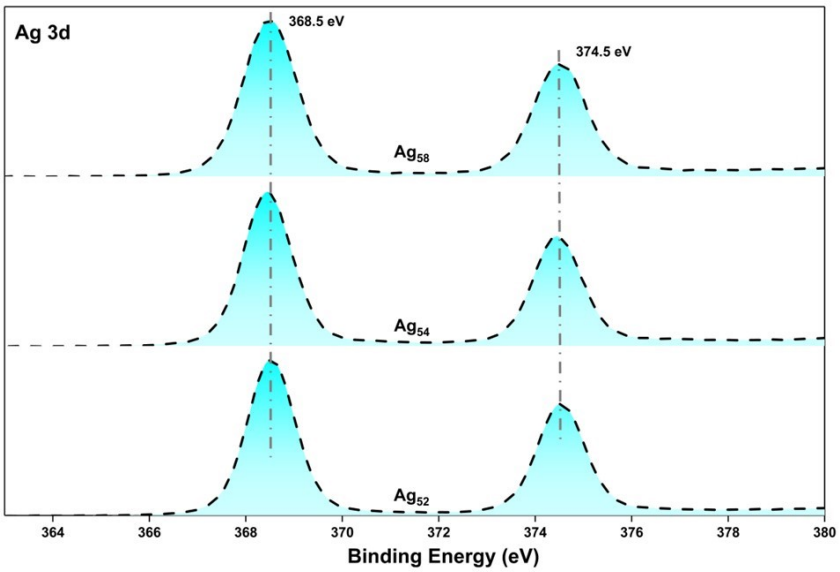

Figure S13. Comparison of the Ag 3d XPS signals of Ag_{52}, Ag_{54}, Ag_{58} nanoclusters. By comparison, the Ag 3d bands of Ag_{52}, Ag_{54}, Ag_{58} nanoclusters are all located at 368.5 and 374.5 eV.

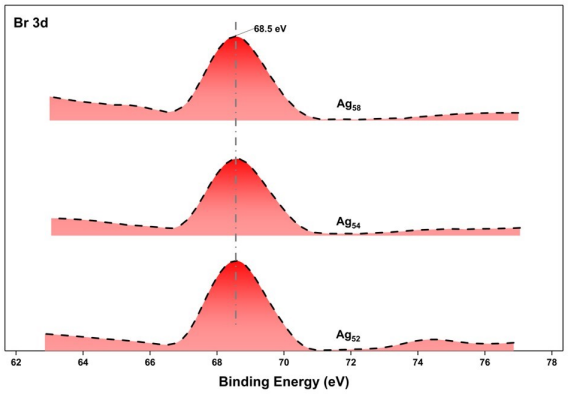

Figure S14. Comparison of the Br 3d XPS signals of Ag_{52}, Ag_{54}, Ag_{58} nanoclusters. By comparison, the Br 3d bands of Ag_{52}, Ag_{54}, Ag_{58} nanoclusters are all located at 68.5 eV.

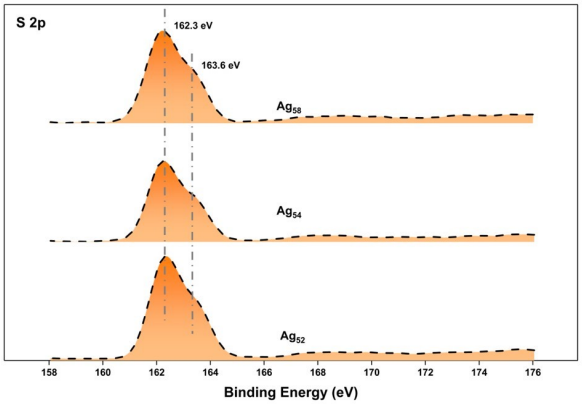

Figure S15. Comparison of the S 2p XPS signals of Ag_{52}, Ag_{54}, Ag_{58} nanoclusters. By comparison, the S 2p bands of Ag_{52}, Ag_{54}, Ag_{58} nanoclusters are all located at 162.3 and 163.6 eV.

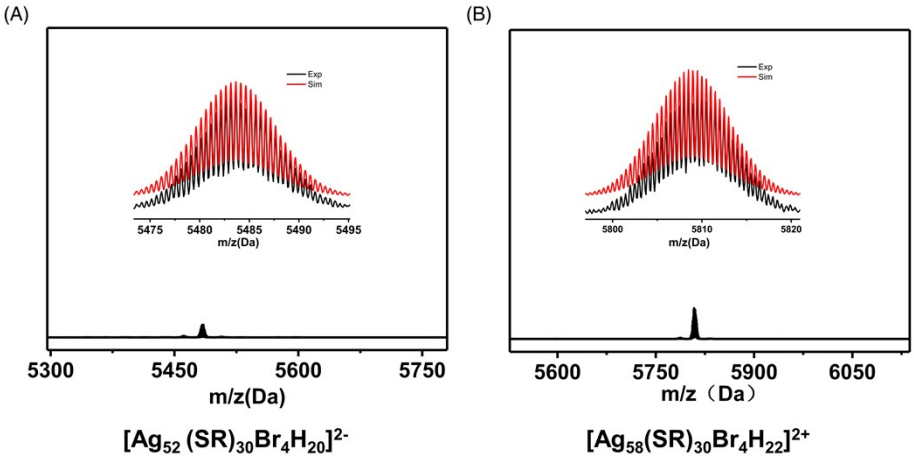

Figure S16. ESI-MS results of (A) $[Ag_{52}(SR)_{30}Br_4H_{20}]^{2-}$ and (B) $[Ag_{58}(SR)_{30}Br_4H_{22}]^{2+}$. Insets in (A,B): experimental (in black) and simulated (in red) isotope patterns of each nanocluster. The nominal electron counts of both nanoclusters were determined as 0e, i.e., 52(Ag) – 30(SR) – 4(Br) – 20(H) + 2(charge) = 0e for $[Ag_{52}(SR)_{30}Br_4H_{20}]^{2-}$ and 58(Ag) – 30(SR) – 4(Br) – 22(H) – 2(charge) = 0e for $[Ag_{58}(SR)_{30}Br_4H_{22}]^{2+}$.

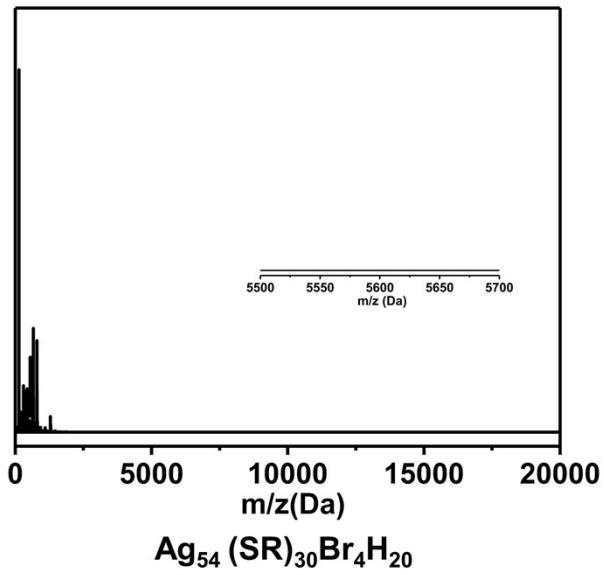

Figure S17. ESI-MS result of the Ag_{54} nanocluster in the negative mode.

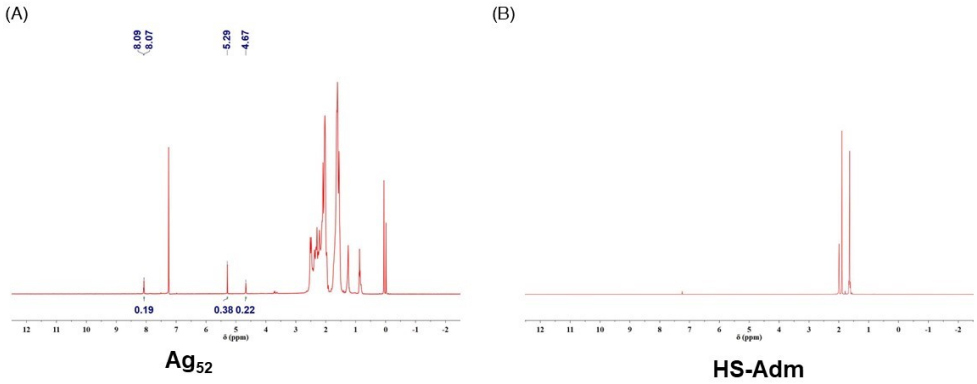

Figure S18. ^{1}H NMR spectra of (A) the Ag_{52} cluster and (B) the HS-Adm ligand.

Table S1. Crystal data and structure refinement for the Ag_{52} nanocluster. The CCDC number of the Ag_{52} nanocluster is 2301182.

Molecular formula	$C_{284}H_{391}Ag_{52}Br_4S_{30}$
Crystal system	orthorhombic
Space group	Pnma
a/Å	47.2631(8)
b/Å	24.0336(3)
c/Å	35.4451(4)
α/°	90
β/°	90
γ/°	90
Volume/Å^3	40262.2(10)
Z	4
ρ_{calc}g/cm^3	1.764
μ/mm^{-1}	21.941
F(000)	20636.0
Radiation	CuKα (λ = 1.54178)
Index ranges	-42 ≤ h ≤ 53, -26 ≤ k ≤ 22, -31 ≤ l ≤ 39
θ range (°)	6.472 -119.998
Measured reflections and unique reflections	65629/29539 [R_{int} = 0.0770, R_{sigma} = 0.1173]
Goodness-of-fit on F^2	1.096
Largest diff. peak/hole / e Å^{-3}	4.85/-4.04
Final R indexes [I>=2σ (I)]	R_1 = 0.1167, wR_2 = 0.2971
Final R indexes [all data]	R_1 = 0.1502, wR_2 = 0.3220

Table S2. Crystal data and structure refinement for the Ag_{54} nanocluster. The CCDC number of the Ag_{54} nanocluster is 2301180.

Molecular formula	$C_{300}H_{449}Ag_{54}Br_4S_{30}$
Crystal system	triclinic
Space group	P-1
a/Å	21.8845(2)
b/Å	22.1526(3)
c/Å	49.1884(4)
α/°	91.5080(10)
β/°	101.2820(10)
γ/°	118.3720(10)
Volume/Å^3	20379.0(4)
Z	2
ρ_{calc}g/cm^3	1.819
μ/mm^{-1}	22.438
F(000)	10814.0
Radiation	CuKα (λ = 1.54186)
Index ranges	-42 ≤ h ≤ 53, -26 ≤ k ≤ 22, -31 ≤ l ≤ 39
θ range (°)	7.988 - 124.998
Measured reflections and unique reflections	168471/63506 [R_{int} = 0.0483, R_{sigma} = 0.0489]
Goodness-of-fit on F^2	1.028
Largest diff. peak/hole / e Å^{-3}	4.09/-4.44
Final R indexes [I>=2σ (I)]	R_1 = 0.0888, wR_2 = 0.2453
Final R indexes [all data]	R_1 = 0.1006, wR_2 = 0.2576

Table S3. Crystal data and structure refinement for the Ag_{58} nanocluster. The CCDC number of the Ag_5 nanocluster is 2301183.

Molecular formula	$C_{300}H_{446}Ag_{58}Br_4N_2O_6S_{30}$
Crystal system	monoclinic
Space group	C2/c
a/Å	38.5120(6)
b/Å	21.9660(4)
c/Å	49.9423(9)
α/°	90
β/°	107.3320(10)
γ/°	90
Volume/Å^3	40330.6(12)
Z	4
ρ_{calc}g/cm^3	1.929
μ/mm^{-1}	24.213
F(000)	22616.0
Radiation	CuKα (λ = 1.54186)
Index ranges	-44 ≤ h ≤ 24, -25 ≤ k ≤ 24, -57 ≤ l ≤ 56
θ range (°)	12.152 -125
Measured reflections and unique reflections	89651/31112 [R_{int} = 0.0639, R_{sigma} = 0.0921]
Goodness-of-fit on F^2	0.986
Largest diff. peak/hole / e Å^{-3}	3.11/-5.14
Final R indexes [I>=2σ (I)]	R_1 = 0.0924, wR_2 = 0.2564
Final R indexes [all data]	R_1 = 0.1261, wR_2 = 0.2868